

# Synthesis and Spectroscopic Characterization of the Copolymers of Aniline and Aniline Derivatives with Poly(ethylene oxide) Chains at the 3-Position

Hyuk-Soo Moon<sup>†</sup> and Jung-Ki Park\*

Department of Chemical Engineering, Korea Advanced Institute of Science and Technology, 373-1, Kusung-dong, Yusung-gu, Daejeon 305-701, Korea

Received January 5, 1998; Revised Manuscript Received May 18, 1998

**ABSTRACT:** The oxidative copolymerization of aniline and anilines derivatized at the 3-position with three different lengths of poly(ethyleneoxy) carboxylate groups was performed. The electric conductivities of the copolymers, measured by the four-point probe method, decreased as the content of aniline derivatives or the graft degree of bulky substituents in the copolymers increased. The more prominent conductivity drop was observed for the copolymer with the longer substituent at a given graft degree. Moreover, an increase in the graft degree of the copolymer induced a blue shift of the absorption bands in the near-IR region and significant line broadening of electron spin resonance signals together with a reduction in spin density. The X-ray diffraction patterns of the copolymer gradually lost the characteristic diffraction peaks of emeraldine hydrochloride as the graft degree of poly(ethylene oxide) (PEO) was increased. The changes in electric and spectroscopic characteristics with the use of PEO side chains on polyaniline backbones were attributed to the steric effects of the substituted poly(ethyleneoxy) carboxylate groups.

## Introduction

A great deal of attention has been focused on  $\pi$ -conjugated organic polymers having benzenoid or heterocyclic units such as poly(*p*-phenylene),<sup>1–3</sup> polythiophene,<sup>4,5</sup> polypyrrole,<sup>6,7</sup> and polyaniline<sup>8,9</sup> as electrical conducting materials, including the development of new conducting polymers by modification of the monomer.<sup>10–12</sup> However, the long-standing goal of developing an all-polymer battery system suitable for secondary commercial cell applications has not yet been achieved because of the lack of appropriate polymer electrodes.

The practical secondary lithium polymer batteries under development are generally of the following type:  $-\text{Li}/\text{polymer electrolyte (Li}^+)/\text{cathode}+$ . The currently used cathodes are metallic oxides such as  $\text{Mn}_2\text{O}_4$  or  $\text{V}_6\text{O}_{13}$  with  $\text{Li}^+$  intercalated into the van der Waals gaps. Cathodes based on conducting polymers usually show poor capacities so that the available power from their electrochemical systems is insufficient for practical application. Higher current capability requires faster redox switching, which in polyaniline is often associated with the transport of both anions and cations inside the polymer matrix.<sup>10</sup> Greater reversibility of the redox system can thus be expected if the ionic conductivity of polyaniline is enhanced without sacrificing its electronic properties. In this regard, the interfacial characteristics of lithium polymer batteries may be significantly improved by using mixed ionic and electronic conducting polymers as the electrodes of such cells, since the interface between the electronically conducting polymer and the polymer electrolyte presents a substantial barrier.<sup>13</sup>

In this work, we tried to minimize this barrier by using an electrode of functionalized polyaniline in which poly(ethyleneoxy) carboxylate chains are grafted onto

the 3-positions of the aniline. The covalent graft of the ether chains on the conjugate system is expected to affect both the electronic and the ionic conductivity. This concept is of great potential interest for the design of ion-selective electrodes or for interfacing conducting polymers with ionic conductors such as poly(ethylene oxide) (PEO) in all-solid-state batteries.<sup>14–20</sup>

We report here a new synthetic method for anilines substituted at the 3-position with a polyether functionality. Interest in this synthetic path arises from recent proposals for the use of *p*-aminobenzoyl chloride in block polyaniline copolymers preparation, reported by Suzhen Li et al.<sup>18</sup> We also present the results for oxidative copolymerization of aniline and PEO-substituted anilines. The electrical properties of the copolymers and their spectroscopic characteristics are reported.

## Experimental Section

**Materials.** Aniline, 3-aminobenzoic acid, diethylamine, and triphenyl methyl chloride (Aldrich, reagent grade) were used as supplied. Tetrahydrofuran (THF) (Merck, HPLC grade), used as the solvent for monomer synthesis, was purified by distillation and stored under nitrogen. Poly(ethylene glycol) methyl ethers ( $M_n$  350, 550, and 750), purchased from Aldrich, were vacuum-distilled prior to use. All other reagents and solvents (reagent grade) were used as received without further purification.

**Synthesis of the PEO-Substituted Anilines and Poly(ethyleneoxy)-3-aminobenzoate (PEAB).** Most procedures for the preparation of the monomers were carried out according to published methods,<sup>21,22</sup> with modifications. The key intermediate for the monomer synthesis, triphenyl methyl (or trityl) 3-aminobenzoyl chloride, was prepared by the base-catalyzed substitution of the amino group in 3-aminobenzoic acid by trityl chloride and subsequent chlorination of the benzoic acid group by thionyl chloride. To a 500-mL glass reactor fitted with a mechanical stirrer, a condenser, and a nitrogen inlet were added 10 g (72.9 mmol) of 3-ami-

\* To whom correspondence should be addressed. Tel: 82-42-869-3925. Fax: 82-42-869-3910. E-mail: pjksorak@kaist.ac.kr.

<sup>†</sup> Current address: LG Cable Research Institute, 555, Hoge, Anyang, Kyungki, 431-080, Korea.

nobenzoic acid, 21 g (75.3 mmol) of triphenyl methyl chloride, 300 mL of THF, and 20 mL (193.4 mmol) of diethylamine. The solution was stirred for 1 h, and then an equivalent amount (72.9 mmol) of the poly(ethylene glycol) methyl ether was added. After heating the solution to the reaction temperature of 60 °C, we added a little excess (~100 mmol) of thionyl chloride and vigorously stirred the mixture for another 3–4 h. The reaction mixture was allowed to cool, a small amount of hydrochloric acid was added to remove the triphenyl methyl group, and the organic insoluble diethylamine·HCl salt was filtered out. The solvent was evaporated, and the resulting crude viscous liquid was dissolved in water, filtered several times, and evaporated again to give PEAB as a brownish viscous liquid or slurry, depending on the molecular weight of the poly(ethyleneoxy) carboxylate group. Three different PEABs were obtained by changing the molecular weights of the poly(ethylene glycol) methyl ethers reacted with 3-aminobenzoic acid.

**Oxidative Copolymerization.** Oxidative copolymerizations of aniline with PEABs were performed similarly to the oxidative homopolymerization of aniline already reported.<sup>23</sup> 5–20 mmol of PEAB, 200 mL of 1 M HCl aqueous solution, and 18.24 g (80 mmol) of ammonium persulfate were mixed in the glass reactor under nitrogen atmosphere. To this solution aniline (60–75 mmol) in 1M HCl solution was added dropwise over a period of 30 min with vigorous stirring. The slow addition of aniline to the PEAB and oxidant solution was essential for preventing the homopolymerization of aniline. The precipitates obtained were washed thoroughly with water/methanol several times to remove any residual poly(PEABs) and dried in a vacuum at 50 °C to give PEO-grafted polyaniline hydrochlorides. The resulting products were then converted to base-type PEO-grafted polyaniline copolymers by treatment with 0.5 M aqueous NH<sub>4</sub>OH, followed by ultracentrifuging, washing with water several times, and drying under vacuum at 40 °C for 2 days.

**Characterization of PEABs and Copolymers.** The PEABs and graft copolymers obtained were characterized by <sup>1</sup>H NMR with a Bruker-AMX-500 NMR spectrometer. For the experiment, we prepared the solutions with polymer concentrations of 0.1 g/cm<sup>3</sup> in a 5-mm (o.d.) glass tube by dissolving the polymers in dimethyl sulfoxide-d<sub>6</sub>. Thermal analysis was also carried out under nitrogen atmosphere with a DuPont Thermal Analyst model 2000 differential scanning calorimeter to study the thermal properties of the synthesized copolymers such as glass transition temperatures and crystallinities.

**Conductivity Measurement.** Electrical dc conductivity of the compressed pellets of the HCl-doped copolymers was measured by the conventional four-point probe technique at room temperature, where the four points in the sample surface were in line at an equal spacing of 1 mm. During the measurements, an appropriate constant current in the range 1–50 μA was applied to the two outer probes, and the voltage drop across the two inner probes was measured to determine the conductivity. The current was supplied by a Keithly model 220 constant current source, and the voltage drop was measured with a Keithly model 182 sensitive digital voltmeter. All pellets used in this experiment were vacuum-dried overnight to minimize the effect of moisture on conductivity.

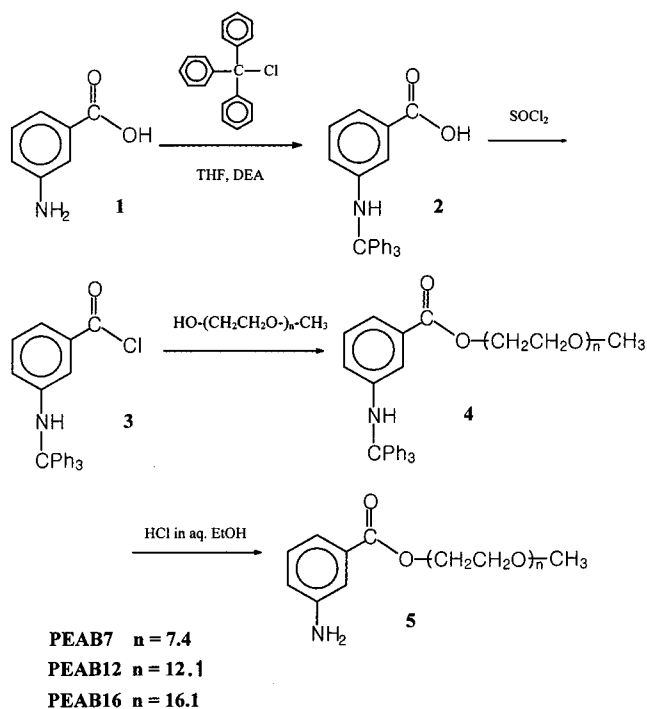


**Figure 1.** Synthesis route of poly(ethyleneoxy)-3-aminobenzoate.

**UV–Vis–Near-IR Spectroscopy.** A UV–vis–near-IR recording spectrophotometer (Shimadzu model UV-3100S) was used to measure optical absorbance in the wavelength range 250–1600 nm of the thin solid films of the (±)-10-camphorsulfonic acid (CSA)-doped and undoped copolymers. To make thin films, the base forms of the copolymers were dissolved to 1% in *N*-methylpyrrolidinone (NMP), or in NMP containing the calculated amount of CSA to make equimolar ratios of CSA to aniline units in the copolymers, and then were coated onto glass plates.

**Electron Spin Resonance (ESR).** The ESR measurements of the HCl-doped copolymers were carried out with a Bruker-EMX-300 spectrometer. The *g* value and spin density were determined by using the signal of 1,1-diphenyl-2-picrylhydrazyl (DPPH) free radical as the standard. To determine the spin density, the intensity of the double-integral ESR spectra for the 0.5 wt % polymer concentration in KBr was compared with that of DPPH at the same concentration. These ESR measurements were carried out under vacuum to avoid the influence of the oxygen adsorption.

**X-ray Diffraction (XRD).** XRD patterns for the HCl-doped and undoped copolymers were obtained with the Rigaku model D/MAX-3C X-ray generator to examine chain ordering of polyaniline backbones in the copolymers. The X-ray beam was nickel-filtered Cu Kα radiation from a sealed tube operated at 40 kV and 45 mA. Data were obtained from 5° to 45° (2θ) at a scan rate of 2°/min.

## Results and Discussion

**Synthesis of the PEO-Substituted Anilines.** Figure 1 shows the synthetic scheme and intermediate structures for the anilines (PEAB7, PEAB12, and PEAB16) containing an polyether chain (average  $n = 7.4, 12.1$ , and  $16.1$ , respectively). It also shows the use of the triphenyl methyl (trityl) group as a protective group for amine since the amine group of 3-aminoben-

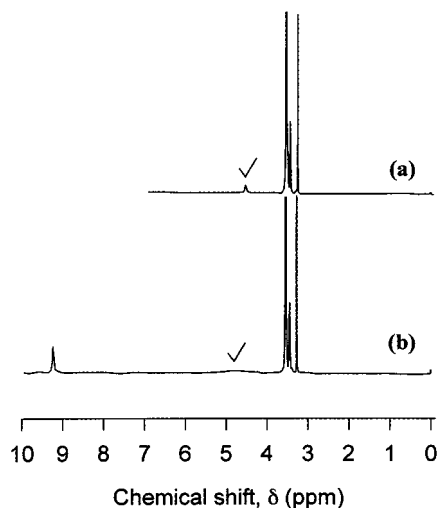


**Figure 2.**  $^1\text{H}$  NMR spectra of (a) poly(ethylene glycol) methyl ether ( $M_n = 350$ ) and poly(ethyleneoxy)-3-aminobenzoate (7 ether linkages).

zoic acid, **1**, easily reacts with the acid chloride to form amides.<sup>21</sup> Because of the low reactivity of the aromatic acid chloride, the reaction of trityl-3-aminobenzyl chloride, **3**, with poly(ethylene glycol) methyl ether was carried out by a modified Schotten–Baumann technique: The thionyl chloride was added in portions to a mixture of the poly(ethylene glycol) methyl ether and diethylamine.<sup>22</sup> Diethylamine was believed not only to neutralize the hydrogen chloride that would otherwise be liberated but also to catalyze the reaction.

Figure 2 shows the representative  $^1\text{H}$  NMR spectra of poly(ethylene glycol) methyl ether of  $M_n = 350$  (PEGME350) and the substituted aniline, PEAB7. The peak for the methylene protons in the PEO chain appeared in two groups, at  $\delta = 3.41\text{--}3.44$  and  $\delta = 3.49\text{--}3.52$ , which could be assigned to the methylene protons adjacent to the methoxy and hydroxy oxides, and to other methylene protons, respectively; the methoxy protons at the PEO chain end resonated somewhat upfield, at  $\delta = 3.25$ .<sup>24</sup> The peak for the hydroxy proton appeared at  $\delta = 4.52$  in the spectrum of PEGME350 (Figure 2a) but was not present in the spectrum of PEAB7 (Figure 2b), which indicates that all the peaks for methylene and methoxy protons in the  $^1\text{H}$  NMR spectrum of PEAB7 originate from the substituted PEO chain, not from the unreacted PEGME350. The phenyl and amine protons of aniline resonated at  $\delta = 9.23$  and  $\delta = 4.3\text{--}5.0$ , respectively (Figure 2b), which is consistent with the molecular structure of PEAB7. The integration ratio of the phenyl protons to methoxy protons was 4:3, which also confirmed the expected structure of PEAB7, shown as **5** in Figure 1.

**Oxidative Copolymerizations.** The oxidative copolymerization of PEABs with aniline gave blue powders in moderate yields. The structural evaluation of the copolymers was made by the  $^1\text{H}$  NMR spectra given in Figure 3. The peaks for the methylene and methoxy protons in the PEO chains of PEABs appeared at  $\delta = 3.2\text{--}3.5$ , whereas the phenyl protons in aniline and PEABs resonated further downfield at  $\delta = 6.8\text{--}7.3$ .<sup>18</sup> From the peak-area ratios of the phenyl protons to those of all other protons at the upper field, we could calculate the PEAB content in poly(aniline-*co*-PEAB).

Table 1 summarizes the compositions and yield of the copolymers, the former being calculated from  $^1\text{H}$  NMR

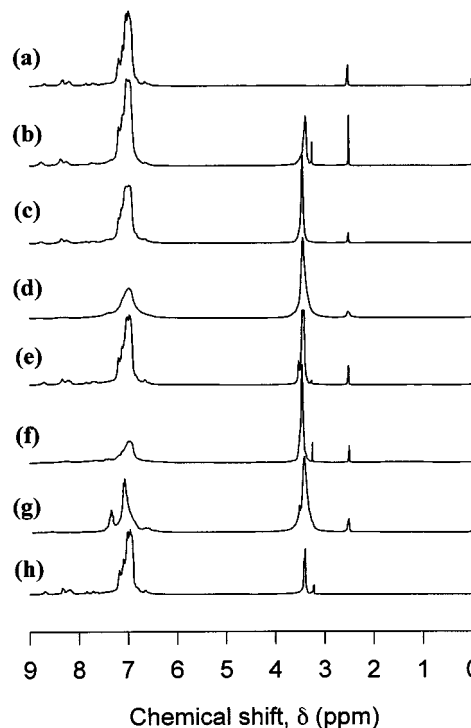


**Figure 3.**  $^1\text{H}$  NMR spectra of (a) polyaniline; (b) 2.3-, (c) 3.3-, (d) 11.5-poly(aniline-*co*-PEAB7); (e) 2.8-, (f) 5.6-, (g) 6.6-poly(aniline-*co*-PEAB12); and (h) 0.8-poly(aniline-*co*-PEAB16).

**Table 1. Compositions and Yields of the PEO-Grafted Polyanilines**

| polymers                                     | feed molar ratio, An:PEAB <sup>a</sup> | composition, An:PEAB | vol% of PEO chain | yield, % |
|--|--|----------------------|-------------------|----------|
| polyaniline                                  | 100:0                                  | 100:0                | 0                 | 85       |
| 2.3 <sup>b</sup> -poly(An- <i>co</i> -PEAB7) | 95:5                                   | 97.7:2.3             | 8.9               | 58       |
| 3.3-poly(An- <i>co</i> -PEAB7)               | 90:10                                  | 96.7:3.3             | 12.3              | 42       |
| 4.8-poly(An- <i>co</i> -PEAB7)               | 85:15                                  | 95.2:4.8             | 17.0              | 33       |
| 5.9-poly(An- <i>co</i> -PEAB7)               | 80:20                                  | 94.1:5.9             | 20.1              | 21       |
| 11.5-poly(An- <i>co</i> -PEAB7)              | 70:30                                  | 88.5:11.5            | 32.9              | 18       |
| 2.8-poly(An- <i>co</i> -PEAB12)              | 90:10                                  | 97.2:2.8             | 15.4              | 33       |
| 5.6-poly(An- <i>co</i> -PEAB12)              | 80:20                                  | 94.4:5.6             | 26.8              | 18       |
| 6.6-poly(An- <i>co</i> -PEAB12)              | 70:30                                  | 93.4:6.6             | 30.2              | 16       |
| 0.8-poly(An- <i>co</i> -PEAB16)              | 90:10                                  | 99.2:0.8             | 6.4               | 23       |

<sup>a</sup> An, aniline. <sup>b</sup> The numerical values stand for mol% of PEAB units in the copolymers, which were determined from the  $^1\text{H}$  NMR spectra.

spectra and the latter estimated gravimetrically from the weight ratios of feed monomers to the synthesized copolymers. Table 1 also shows the vol % of PEO chains in the copolymers, calculated by assuming of the same density for the polyaniline backbone and for the PEO side chains in the graft copolymers. The polymer yields are similar to or slightly higher than those reported for other, similar polymerization systems.<sup>25</sup> The polymer yield decreases as the feed ratio of PEABs increases, which indicates that the presence of bulky substituent, i.e., poly(ethyleneoxy) carboxylate, hinders the formation of head-to-tail coupling during the polymerization reaction. Moreover, the longer the substituent, the lower the polymer yield at a given feed ratio, which again suggests that the polymer yields are strongly affected by the degree of steric hindrance of the substituent. This would be consistent with the recent theoretical studies on unsubstituted polyaniline, which have shown a strong steric interaction between the hydrogen atoms of neighboring rings during the polym-



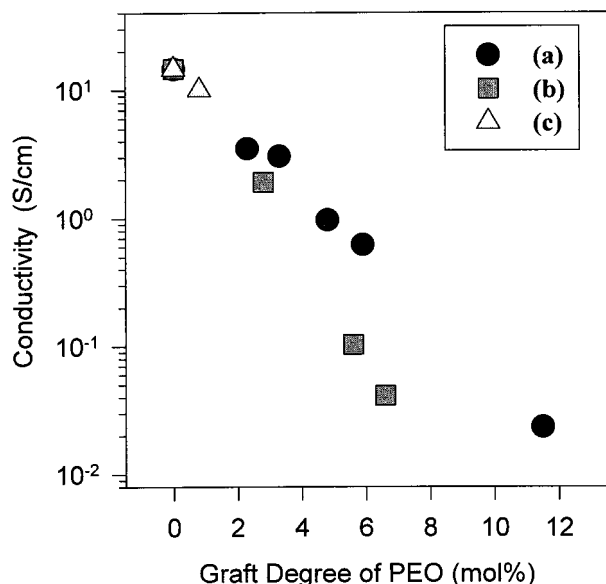


**Figure 4.** Room-temperature dc conductivities of the HCl-doped copolymers versus the graft degree of PEO side chain: (a) poly(aniline-*co*-PEAB7), (b) poly(aniline-*co*-PEAB12), (c) poly(aniline-*co*-PEAB16).

erization reaction.<sup>26</sup> Therefore, substitution of the hydrogen atoms by the bulky poly(ethyleneoxy) carboxylate necessarily leads to an increase of the steric hindrance that seems to limit the polymerization processes.

**Electrical Conductivities of the Doped Copolymers.** Figure 4 shows the effects of the copolymer composition, i.e., graft degree of PEO, and the chain length of the grafted PEO on the conductivities of the HCl-doped copolymers. For all three different copolymer series with different lengths of PEO side chains, the conductivities of the HCl-doped copolymers decrease as the graft degree of PEO increases. This reduction of conductivities accompanying the use of PEO side chains can be explained by two kinds of steric effects. The first possible explanation is the conformational steric effect of the substituted poly(ethyleneoxy) carboxylate group, i.e., the PEO side chain, since the substituent may restrict the ring conformation of aniline. Substituting the bulky poly(ethyleneoxy) carboxylate groups on the 3-position of aniline in PEAB may induce ring twisting, i.e., nonplanar conformations, which decreases the  $\pi$  conjugation length along the polyaniline backbone and thus destabilizes the polysemiquinone radical cation and gives higher redox potentials. This kind of explanation for the reduction of conductivity of the substituted polyaniline has been reported in the literature for various polyaniline derivatives.<sup>16</sup>

The other possible explanation for the reduction of conductivities with the use of a PEO-grafted chain, which is electrically nonconductive, is the intermolecular steric effect. The bulky substituted groups may also reduce the intermolecular contacts between the neighboring polyaniline backbones through their steric effect, and hence induce a disorder in chain separations within the metallic conduction region of the copolymer. Considering the conduction mechanism of polyaniline, the reduction of interchain contact is indicative of the shortening of coherence length between the neighboring polyaniline backbones; thus the electrons in the polaronic lattice in polyaniline are confined to segments of a chain and become localized. This confinement and

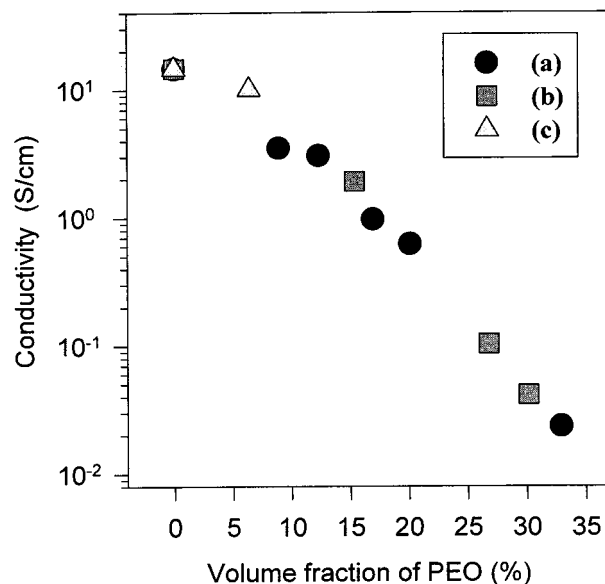


**Figure 5.** Room-temperature dc conductivities of the HCl-doped copolymers versus the volume fraction of PEO side chain: (a) poly(aniline-*co*-PEAB7), (b) poly(aniline-*co*-PEAB12), (c) poly(aniline-*co*-PEAB16).

localization of electrons may reduce the interchain diffusion rate of electrons and therefore lead to the decrease of conductivity. Similar arguments have been reported by us for the polymeric acid-doped polyaniline systems<sup>27,28</sup> and by others for poly(*o*-toluidine)<sup>29</sup> and poly(3-alkylthiophenes).<sup>30</sup>

Interestingly, the degree of conductivity drop with the graft degree of PEO is different among the copolymers with the different PEO chain lengths (Figure 4). Though the conductivities of the PEO-grafted polyanilines are decreased with the increase of the graft degree, a more significant conductivity loss is observed for the copolymer with the longer PEO side chain at a given graft degree. This result may be explained by the difference in the degree of the aforementioned intermolecular steric effect of the copolymers with different lengths of PEO side chains, since the longer PEO chain should reduce the interchain contact of polyanilines more. To confirm our explanation, the conductivity of the PEO grafted polyanilines are replotted in Figure 5 as a function of the volumetric content of the (electrically nonconductive) PEO chains. This clearly shows that the conductivity loss of the copolymers is strongly dependent on the volumetric content of PEO in the copolymers. Considering the nature of the two steric effects mentioned above, the intermolecular steric effect seems to depend more strongly on the volumetric content of the insulating PEO, whereas the conformational effect depends more on the number of substitution sites. Therefore, the intermolecular steric effect seems to be more important than the conformational effect in the loss of conductivity of the PEO-grafted polyanilines, at least within the graft degree range investigated in this study.

**Chain Conformations and Polaron Formations of the Copolymers.** The UV-vis spectra of the undoped polyaniline and PEO-grafted polyanilines are given in Figure 6. The UV-vis spectrum of the polyaniline has two absorption peaks, at 324 and 639 nm, which originate from the  $\pi-\pi^*$  transition of the benzenoid rings and the exciton absorption of the quinoid rings,<sup>25,31</sup> respectively. For all three PEO-grafted poly-

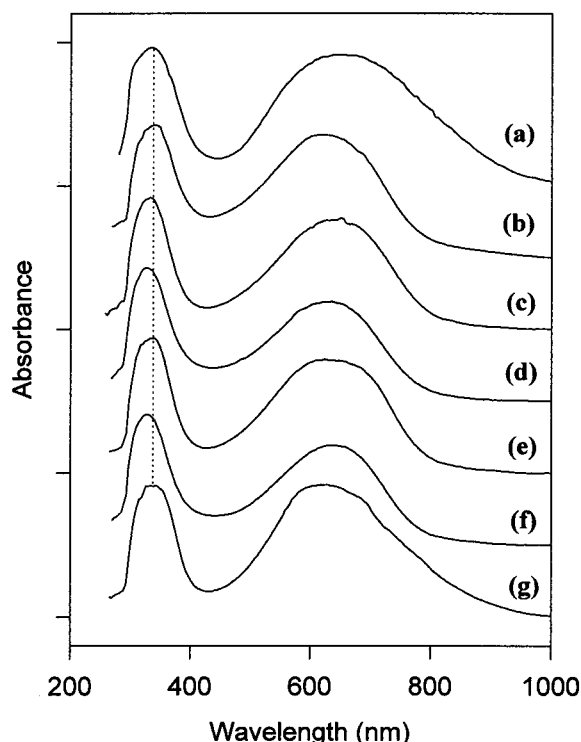


**Figure 6.** UV-vis-near-IR absorption spectra of the undoped (a) polyaniline; (b) 3-, (c) 5.9-, (d) 11.5-poly(aniline-co-PEAB7); (e) 2.8-, (f) 6.6-poly(aniline-co-PEAB12); and (g) 0.8-poly(aniline-co-PEAB16).

aniline series with different PEO lengths, the benzenoid absorption peaks exhibit blue shifts, the shift becoming greater as the graft degree of PEO increases. These blue shifts of the benzenoid absorption peaks indicate the nonplanar conformation of the polymer backbone, since a more-distorted ring conformation is indicative of the reduction of conjugation length or the blue shift of the absorption peak. Leclerc et al.<sup>16</sup> and Bredas et al.<sup>32</sup> also have reported that certain substituents can induce some nonplanar conformations that decrease the conjugation length (viz., decrease the absorption maximum) along the polymer backbone and thus give higher redox potentials. Therefore, this blue shift of the benzenoid absorption peak and the greater shift for the higher graft degree are related to the higher torsion angle in the PEO-grafted polyanilines compared with polyaniline itself, which supports the concept of the conformational steric effect of the substituted PEO chains.

Figure 6 shows another interesting result. Not only is the peak location of benzenoid absorption at  $\sim 320$  nm blue-shifted but also the peak intensity of the exciton absorption at  $\sim 630$  nm is decreased as the graft degree of PEO increases. Moreover, the high-wavelength regime of the exciton absorption peak is suppressed in the spectra of the PEO-grafted polyanilines compared with the spectrum of polyaniline (Figure 6a). This indicates the molecular conformations of the polyaniline and the PEO-grafted polyanilines differ from each other; that is, when they are cast from NMP solutions, the PEO-grafted polyanilines are more compact coils than is the pristine polyaniline. Based on the results reported by Angelopoulos et al.,<sup>33</sup> who observed a significant red shift (620 to 648 nm) in the exciton peak of polyaniline processed with LiCl that might disrupt the inter- and intrachain interactions, this blue shift and intensity

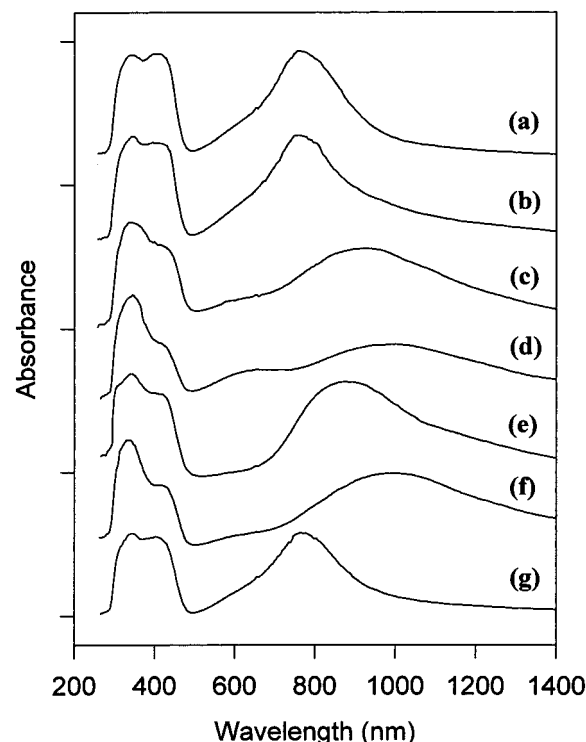


**Figure 7.** UV-vis-near-IR absorption spectra of the CSA-doped (a) polyaniline; (b) 3-, (c) 5.9-, (d) 11.5-poly(aniline-co-PEAB7); (e) 2.8-, (f) 6.6-poly(aniline-co-PEAB12); and (g) 0.8-poly(aniline-co-PEAB16).

reduction of the exciton absorption peak in the PEO-grafted polyaniline can be explained as follows: In general, some form of aggregation or clumping is believed to occur in the polyaniline chains dissolved in NMP, accounting for the exhibition of the bimodal gel-permeation chromatography curves of polyaniline base in NMP.<sup>33–35</sup> The aggregation is thought to result from the strong interchain interactions such as physical entanglements or hydrogen bonding with the help of the NMP.<sup>9,35,36</sup> The aggregation may be enhanced by the use of PEO, since the more polar PEO chain can enhance the interchain interactions in the presence of the less polar NMP, thus promoting a compact coil conformation. Similar dependency of the molecular conformation on the substitution onto the polyaniline ring has been reported by MacDiarmid and Epstein,<sup>9</sup> who found that poly(*o*-toluidine) behaved the opposite from polyaniline when both polymers were doped with CSA and subsequently treated with *m*-cresol or chloroform. They explained that the partial coating of the doped polar polymer chain with nonpolar, covalent methyl groups permits the chain to interact preferentially with the less polar chloroform than with the more polar *m*-cresol, in contrast to polyaniline, which interacts more readily with the polar *m*-cresol.

In Figure 7 are shown the UV-vis spectra of the CSA-doped polyaniline and PEO-grafted polyanilines. With the CSA doping, no exciton absorption peak is observed except in the polymer 11.5-poly(aniline-co-PEAB7), which was made with the highest graft degree of PEO in this study. The absorption spectrum of the doped 11.5-poly(aniline-co-PEAB7) (Figure 7d) shows a small trace of exciton absorption at 620 nm. The UV spectra of the doped copolymers show a characteristic polaron peak at 430 nm and a localized polaron absorption peak at 790 nm for polyaniline<sup>33</sup> and copolymers with low

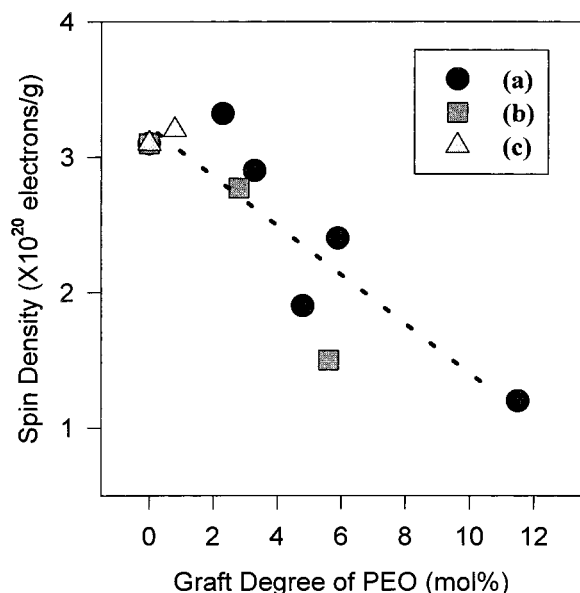


**Figure 8.** Dependence of spin densities of the HCl-doped (a) poly(aniline-*co*-PEAB7), (b) poly(aniline-*co*-PEAB12), and (c) poly(aniline-*co*-PEAB16) on the graft degree of the PEO side chain. The dotted line is the first-order regression of all the data.

graft degree (Figures 7a, 7b, 7e, and 7g) or a weak polaron absorption peak at 1000–1100 nm for copolymers with a relatively high graft degree (Figures 7c, 7d, and 7f). Moreover, the polaron peak at 430 nm is weaker for the copolymers with lower graft degree,<sup>28</sup> which is indicative of the less metallic behavior. These results indicate that the PEO interferes with the doping and consequently with the polaron formation. The poorer polaron formation of the copolymers with the higher graft degree of PEO is consistent with the conductivity behavior of the copolymers and gives another explanation for the conductivity decrease of polyaniline with the addition of PEO side chains. Watanabe et al. reported similar results for the poly(*N*-alkylaniline)s, where the poorer polaron formation was observed with the bulkier alkyl group substitution.<sup>15</sup>

The ESR experiment also confirms the phenomenon of poorer polaron formation with higher graft degree in the PEO-grafted polyanilines. Figure 8 shows the spin density of the HCl-doped polyaniline and the copolymers obtained from the double-integration of their ESR spectra. The spin density tends to decrease with the increase of graft degree, which is well consistent with the UV-vis spectra in Figure 7 and suggests that the reduction of conductivity of the PEO-grafted polyaniline in comparison with polyaniline can be explained by the poorer polaron formation as well as the steric effect of the substituted PEO chains. However, even the lowest spin density of the PEO-grafted polyanilines is more than one-third of the spin density of polyaniline, which indicates that the difference of up to about 3 orders of magnitude in conductivity between polyaniline and the PEO-graft polyaniline cannot be explained by only the spin density difference. Therefore, the steric effect of the substituted PEO chains should necessarily be considered in explaining the conductivity drop with the introduction of PEO chains.

Figure 9 shows ESR spectra of the copolymers, which were measured in powdered samples without dilution; the line widths,  $\Delta H$ , and  $g$  values obtained from the ESR

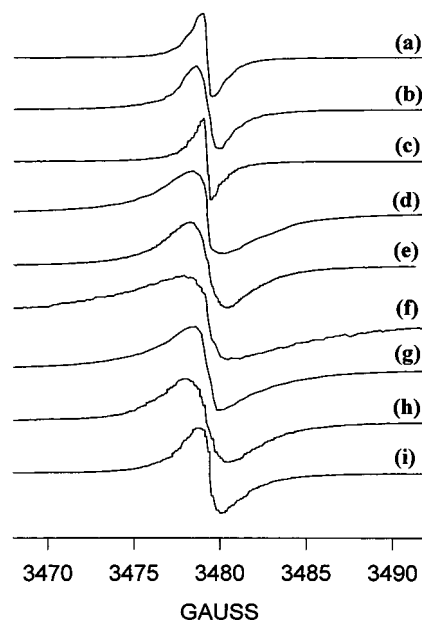


**Figure 9.** ESR spectra of the HCl-doped (a) polyaniline; (b) 2.3-, (c) 3.3-, (d) 4.8-, (e) 5.9-, (f) 11.5-poly(aniline-*co*-PEAB7); (g) 2.8-, (h) 5.6-poly(aniline-*co*-PEAB12); and (i) 0.8-poly(aniline-*co*-PEAB16).

**Table 2.** ESR Parameters of Polyaniline and PEO-Grafted Polyanilines

| sample                               | $g$ value | $\Delta H$ , G |
|--------------------------------------|-----------|----------------|
| polyaniline                          | 2.0077    | 0.89           |
| 2.3-poly(aniline- <i>co</i> -PEAB7)  | 2.0057    | 1.17           |
| 3.3-poly(aniline- <i>co</i> -PEAB7)  | 2.0077    | 0.85           |
| 4.8-poly(aniline- <i>co</i> -PEAB7)  | 2.0086    | 1.74           |
| 5.9-poly(aniline- <i>co</i> -PEAB7)  | 2.0064    | 2.26           |
| 11.5-poly(aniline- <i>co</i> -PEAB7) | 2.0079    | 2.96           |
| 2.8-poly(aniline- <i>co</i> -PEAB12) | 2.0058    | 1.99           |
| 5.6-poly(aniline- <i>co</i> -PEAB12) | 2.0074    | 2.61           |
| 0.8-poly(aniline- <i>co</i> -PEAB16) | 2.0067    | 1.40           |

spectra are summarized in Table 2. The  $g$  values of the polyaniline and copolymers are similar to or slightly greater than that of DPPH (2.0046), which indicates that the unpaired electrons are located on a tertiary amine nitrogen.<sup>6,37</sup> The line widths of polyaniline, and of 2.3- and 3.3-poly(aniline-*co*-PEAB7), are quite narrow even in comparison with that of DPPH, which is a typical example for spin-exchange narrowing caused by the high density of spin ( $\Delta H = 1.3$  G). On the other hand, the line width of the ESR spectra of whole copolymers shows a moderate tendency to increase with the increasing graft degree of PEO chains. Since the spin-exchange interaction is one of the main reasons for the narrowing of the ESR spectrum, the increasing tendency of line width with the increasing graft degree of PEO can be attributed to the decrease of spin density (Figure 9 and Table 2). Another possible reason for the line-width broadening with the increase of the graft degree is the reduction of spin diffusion in the polyaniline backbone by the intermolecular steric effect of the substituted PEO chains, as mentioned before. Recently, Glarum and Marshall<sup>38</sup> suggested the three-dimensional spin diffusion in polyaniline on the basis of the ESR line shapes, and Watanabe et al.<sup>15</sup> invoked the concept of highly diffusive spin to explain the line-width broadening of poly(*N*-alkylaniline)s compared with polyaniline.

**Molecular Alignments of PEO Side Chain and Polyaniline Backbone in the Copolymers.** The

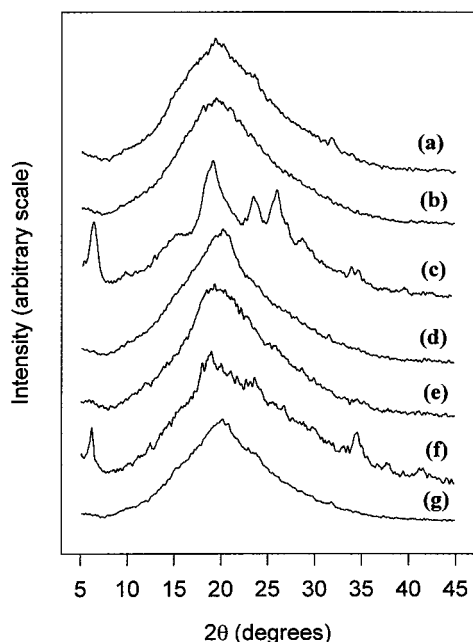


**Figure 10.** X-ray diffraction patterns of the undoped (a) polyaniline; (b) 3.3-, (c) 11.5-poly(aniline-*co*-PEAB7); (d) 2.8-, (e) 5.6-, (f) 6.6-poly(aniline-*co*-PEAB12); and (g) 0.8-poly(aniline-*co*-PEAB16).

XRD results also give valuable information about the correlation between the electric conductivity and the polymer structure. In Figure 10, the XRD patterns of the undoped copolymers are given. All the XRD spectra of the copolymers except for the copolymers with high graft degree, i.e., 11.5-poly(aniline-*co*-PEAN7) and 5.6-poly(aniline-*co*-PEAB12), show a typical X-ray pattern of dedoped polyaniline.<sup>39</sup> They consist mainly of one intense broad peak at  $2\theta \approx 20^\circ$  ( $d \sim 4.6$  Å), which is characteristic of the diffraction by an amorphous polymer. The highly grafted copolymers show considerable diffraction peaks at  $2\theta \approx 19^\circ$ ,  $24^\circ$ ,  $27^\circ$ , and  $35^\circ$  (Figs. 10c and 10f), which are similar to the characteristic diffraction peaks of high-molecular-weight PEO.<sup>40</sup> Differential scanning calorimetry (DSC) results also show that small endothermic peaks at  $\sim 30^\circ\text{C}$  appear in 11.5-poly(aniline-*co*-PEAB7) and 5.6-poly(aniline-*co*-PEAB12) (Figs. 11a and 11c), which indicates that some amount of crystallines of PEO side chains exist in the highly grafted polyanilines. Though the low-molecular-weight PEGME 350 cannot maintain crystalline structure at room temperature where the XRD patterns were obtained, the XRD patterns and the DSC results show that the substituted PEO with the same molecular weight maintains considerable crystallinity at room temperature. This could be explained by the free volume loss of the substituted PEO since the substituted PEO is bound at one end onto an aniline ring and needs more thermal energy to overcome the lattice energy of its crystal and hence fuses at a higher temperature than the unbound PEGME 350.

Figure 12 shows the XRD patterns of the HCl-doped polyaniline and copolymers. The XRD pattern of polyaniline (Figure 12a) clearly shows the characteristic diffraction peaks of emeraldine hydrochloride at  $2\theta \approx 10^\circ$ ,  $16^\circ$ ,  $21^\circ$ , and  $25^\circ$ <sup>39</sup>; these diffraction peaks gradually diminish as the graft degree of PEO increases for all the three copolymer series with different lengths of PEO. This suggests that the polyaniline backbone alignment is hindered by the PEO side chains, which

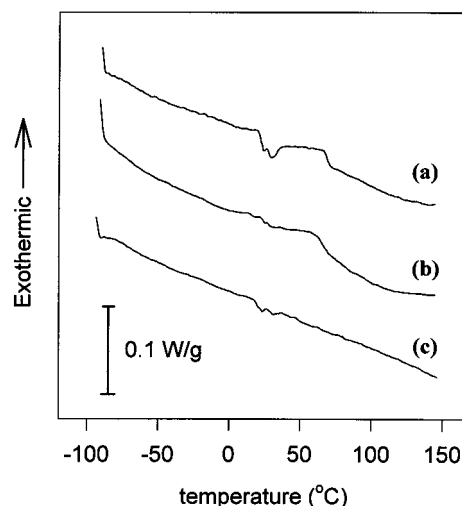


**Figure 11.** DSC thermograms of (a) 11.5-poly(aniline-*co*-PEAB7), (b) 2.8-poly(aniline-*co*-PEAB12), and (c) 5.6-poly(aniline-*co*-PEAB12) at a heating rate of  $10^\circ\text{C}/\text{min}$ .

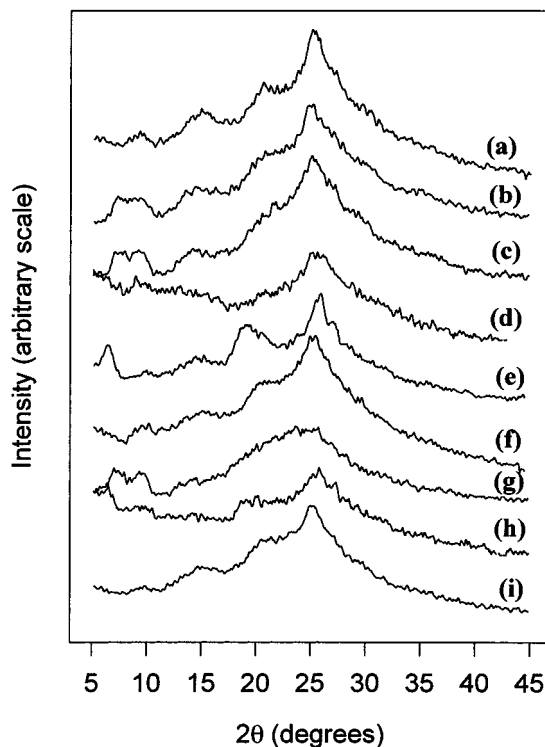


**Figure 12.** X-ray diffraction patterns of the HCl-doped (a) polyaniline; (b) 2.3-, (c) 3.3-, (d) 5.9-, (e) 11.5-poly(aniline-*co*-PEAB7); (f) 2.8-, (g) 5.6-, (h) 6.6-poly(aniline-*co*-PEAB12); and (i) 0.8-poly(aniline-*co*-PEANB16).

strongly supports again the concept of the intermolecular steric effect of the substituted PEO chains. The XRD patterns of the copolymers with a high graft degree of PEO, i.e., 11.5-poly(aniline-*co*-PEAB7) and 5.6-poly(aniline-*co*-PEAB12), still show some trace of diffraction peaks that are believed to originate from the crystalline of PEO side chains, even after those copolymers are doped with HCl (Figures 12e and 12h).

## Conclusion

Monomeric aniline derivatized at the 3-position with a poly(ethyleneoxy) group separated from the aniline ring by a carboxylate group was newly synthesized. The copolymers of aniline and PEO-substituted aniline



have also been synthesized by oxidative polymerization. The conductivity of the doped copolymers decreased with increasing the graft degree of PEO, which is closely correlated with the spectroscopic data. As the absorption band of benzenoid, which corresponds to the conjugation length, was shifted to lower wavelength, the conductivity decreased. This blue shift was attributed to the conformational steric effect of the substituent, i.e., the PEO chain, which might induce nonplanar conformation of aniline ring. The line width of the ESR spectrum also showed a correlation with the conductivity, the conductivity decreasing with an increase of the line width. This line broadening was attributed to the intermolecular steric effect of the substituent, which confines the electron and reduces spin diffusion, and to the spin-density reduction, which corresponds to the poor polaron formation. The XRD peaks were gradually diminished with the decrease of conductivity, which was also attributed to the intermolecular steric effect of substituents that would interfere with the chain alignment of polyaniline backbone.

## References and Notes

- (1) Kido, J. *TRIP* **1994**, 2, 350.
- (2) Gustafsson, G.; Cao, Y.; Treacy, G. M.; Klavetter, F.; Colaneri, N.; Heeger, A. J. *Nature* **1992**, 357, 477.
- (3) Berggren, M.; Inganäs, O.; Gustafsson, G.; Rasmussen, J.; Andersson, M. R.; Hjertberg, T.; Wennerström, O. *Nature* **1994**, 372, 444.
- (4) Roncali, J.; Li, H. S.; Garreau, R.; Garnier, F.; Lemaire, M. *Synth. Met.* **1990**, 36, 267.
- (5) Polis, D. W.; Young, C. L.; McLean, M. R.; Dalton, L. R. *Macromolecules* **1990**, 23, 3231.
- (6) Moon, D. K.; Padias, A. B.; Hall, H. K., Jr.; Huntoon, T.; Calvert, P. D. *Macromolecules* **1995**, 28, 6205.
- (7) Ferloni, P.; Mastragostino, M.; Meneghello, L. *Electrochim. Acta* **1996**, 41, 27.
- (8) Genies, E. M.; Boyle, A.; Lapkowski, M.; Tsintavis, C. *Synth. Met.* **1990**, 36, 139.
- (9) MacDiarmid, A. G.; Epstein, A. J. *Synth. Met.* **1995**, 69, 85.
- (10) Bruce, P. G., Ed. *Solid State Electrochemistry*; Cambridge University Press: Cambridge, U.K., 1995.
- (11) Lipkowski, J.; Ross, P. N., Eds. *Electrochemistry of Novel Materials—Frontiers of Electrochemistry*; VCH Publishers: New York, 1994.
- (12) Chilton, J. A.; Goosey, M. T., Eds. *Special Polymers for Electronics & Optoelectronics*; Chapman & Hall: London, 1995.
- (13) Novak, P.; Inganäs, O.; Björklund, R. *J. Power Sources* **1987**, 21, 17.
- (14) Roncali, J.; Li, H. S.; Garnier, F. J. *Phys. Chem.* **1991**, 95, 8983.
- (15) Watanabe, A.; Mori, K.; Iwabuchi, A.; Iwasaki, Y.; Nakamura, Y. *Macromolecules* **1989**, 22, 3521.
- (16) Leclerc, M.; Daperno, G.; Zotti, G. *Synth. Met.* **1993**, 55–57, 1527.
- (17) Fabrizio, M.; Mengoli, G.; Musiani, M. M.; Paolucci, F. *Synth. Met.* **1991**, 44, 271.
- (18) Li, S.; Dong, H.; Cao, Y. *Synth. Met.* **1989**, 29, E329.
- (19) Chapman, S. E.; Billingham, N. C.; Armes, S. P. *Synth. Met.* **1993**, 55–57, 995.
- (20) Wang, Y.; Rubner, M. F. *Macromolecules* **1992**, 25, 3284.
- (21) Mackie, R. K.; Smith, D. M.; Aitken, R. A. *Guidebook to Organic Synthesis*; Longman Scientific & Technical: Essex, U.K., 1990.
- (22) Morrison, R. T.; Boyd, R. N. *Organic Chemistry*; Allyn and Bacon: Needham Heights, MA, 1987.
- (23) MacDiarmid, A. G.; Epstein, A. J. *Faraday Discuss., Chem. Soc.* **1989**, 85, 317.
- (24) Pouchert, C. J.; Behnke, J., Eds. *The Aldrich Library of <sup>13</sup>C and <sup>1</sup>H FT NMR Spectra*; Aldrich Chemical Co.: Milwaukee, WI, 1993.
- (25) Dao, L. H.; Leclerc, M.; Guay, J.; Chevalier, J. W. *Synth. Met.* **1989**, 29, E377.
- (26) Langer, J. J. *Synth. Met.* **1987**, 20, 35.
- (27) Moon, H. S.; Park, J. K. *J. Polym. Sci., Polym. Chem. Ed.* **1998**, 36, 1431.
- (28) Moon, H. S.; Park, J. K. *Synth. Met.* **1998**, 29, 223.
- (29) Wang, Z. H.; Ehrenfreund, E.; Ray, A.; MacDiarmid, A. G.; Epstein, A. J. *Mol. Cryst. Liq. Cryst.* **1990**, 189, 263.
- (30) Roncali, J.; Garreau, R.; Yassar, A.; Marque, P.; Garnier, F.; Lemaire, M. *J. Phys. Chem.* **1987**, 91, 6706.
- (31) Stafstrom, S.; Bredas, J. L.; Epstein, A. J.; Woo, H. S.; Tanner, D. B.; Huang, W. S.; MacDiarmid, A. G. *Phys. Rev. Lett.* **1987**, 59, 1464.
- (32) Bredas, J. L.; Street, G. B.; Themans, B.; Andre, J. M. *J. Chem. Phys.* **1985**, 83, 1323.
- (33) Angelopoulos, M.; Liao, Y. H.; Furman, B.; Graham, T. *Macromolecules* **1996**, 29, 3046.
- (34) Wei, Y.; Hsueh, F. K.; Jang, G. W. *Macromolecules* **1994**, 27, 518.
- (35) Wang, F. S.; Jing, X. B.; Wang, X. H.; Dong, A. J. *Synth. Met.* **1995**, 69, 93.
- (36) Adams, P. N.; Monkman, A. P.; Apperley, D. C. *Synth. Met.* **1993**, 55, 725.
- (37) Townshend, A.; Worsfold, P. J.; Haswell, S. J.; Macrae, R.; Werner, H. W.; Wilson, I. D., Eds. *Encyclopedia of Analytical Science*; Academic Press: London, 1995.
- (38) Glarum, S. H.; Marshall, J. H. *J. Electrochem. Soc.* **1987**, 134, 2160.
- (39) Pouget, J. P.; Jozefowicz, M. E.; Epstein, A. J.; Tang, X.; MacDiarmid, A. G. *Macromolecules* **1991**, 24, 779.
- (40) Kim, D. W. Ph.D. Thesis; Korea Advanced Inst. of Sci. and Technol., 1996.

MA980003K